INDONESIAN JOURNAL ON GEOSCIENCE
Geological Agency
Ministry of Energy and Mineral Resources

Journal homepage: https://ijog.geologi.esdm.go.id
ISSN 2355-9314, e-ISSN 2355-9306

Analysis of Stress Ratio and Stress Regime in West Java, Indonesia

Anne M. M. Sirait[1], Kadek H. Palgunadi[2,3], Andrean V. H. Simanjuntak[5], Nadhira Rahmania[1], Izaaz Naufal[1], M. Nanda Rizqi Dhiarofa[1], Akhlaqul Karimah[1], Rafi Sadam AL-Ghifari[1], Azhari Ramadhani[1], Farrastha Hady[1], Dwa Desa Warnana[2], and Wiwit Suryanto[4]

[1]Geophysics, Faculty of Mathematics and Natural Science, Universitas Indonesia, Indonesia
[2]Department of Geophysical Engineering, Faculty of Civil Planning and Geo-Engineering, Institut Teknologi Sepuluh Nopember, Surabaya, Indonesia
[3]Swiss Seismological Service (SED), ETH Zürich, Switzerland
[4]Department of Physics, Universitas Gadjah Mada, Yogyakarta, Indonesia
[5]Indonesian Agency for Meteorology, Climatology, and Geophysics (BMKG), Jakarta, Indonesia

Corresponding author: anne.meylani@ui.ac.id
Manuscript received: November, 27, 2024; revised: June, 23, 2025;
approved: January, 07, 2026; available online: March, 16, 2026

Abstract - This study actively investigates stress ratios, principal stress orientations, and stress regimes in the West Java Province, Indonesia, by simultaneously inverting both the stress tensor and fault orientations from 232 moment tensors. It identifies diverse stress regimes, including normal and reverse faulting in the subduction zone, as well as mixed reverse and strike-slip faults across the island. Stress ratios range from 0.08 to 0.97. Sedimentary basins in the northeast produce lower values, while tectonic forces near the southern subduction zones generate higher values. In the subduction zone, plate bending generates normal faulting, while compressional forces lead to reverse faulting. The fore-arc region exhibits a variety of regimes: normal, reverse, and strike-slip, indicating transitions in the dynamics of subduction. Across the island, a combination of reverse and strike-slip faulting suggests crustal compression, with Mount Anak Krakatau exhibiting evidence of normal faulting. The study uncovers a complex interplay of subduction processes, crustal deformation, and geological heterogeneities. It outlines stress regimes ranging from normal and reverse faulting in the subduction zone to mixed reverse and strike-slip faulting on the island. These findings offer crucial insights into the tectonic processes shaping West Java, and lay the groundwork for more informed seismic hazard assessments and risk mitigation strategies.

Keywords: West Java, tectonic stress, stress ratio, principal stress, iterative joint inversion

How to cite this article:
Sirait, A.M.M., Palgunadi, K.H., Simanjuntak, A.V.H., Rahmania, N., Naufal, I., Dhiarofa, M.N.R., Karimah, A., Al-Ghifari, R.S., Ramadhani, A., Hady, F., Warnana, D.D., and Suryanto, W., 2026. Analysis of Stress Ratio and Stress Regime in West Java, Indonesia. *Indonesian Journal on Geoscience*, 13 (1), p.43-55. DOI: 10.17014/ijog.13.1.43-55

Introduction

Java Island, the most populated island in the world, has endured several major earthquakes over the past century, revealing various types of earthquake faulting, particularly in West Java. Positioned at the transition between the Sumatra oblique subduction zone and Java orthogonal subduction zone (Koulali *et al*., 2017). West Java experiences complex tectonic interactions. Off its coast, Mount Anak Krakatau, an active volcano, further complicates the region geological setting. Tectonic forces and volcanic activity drive complicated crustal deformation around

West Java (Harjono *et al*., 1991). These ongoing crustal changes are critical in redistributing stress and increasing or decreasing the accumulation of strain energy, which ultimately releases during earthquakes. As a result, West Java faces a high risk of seismic hazards, particularly due to its location in a densely populated region.

The tectonic setting of West Java, influenced by subduction dynamics, actively shapes complex stress regimes, including normal, reverse, and strike-slip faulting, as the dominant faulting styles in the region (Koulakov *et al*., 2009). These stress regimes vary spatially due to the combined effects of plate boundary forces, topography, and local geological structures (Zoback, 1992; McCaffrey, 2009). Plate interactions, such as subduction, control large-scale stress patterns by generating compressional (reverse) regimes near convergent margins and extensional (normal) regimes in back-arc areas. Topographic features, including mountains and basins, introduce gravitational stresses that favour normal faulting in elevated areas and strike-slip or reverse faulting along steep gradients. Local structures, such as pre-existing faults, further influence stress orientations by generating mixed regimes or causing stress rotations (Townend and Zoback, 2000; Palgunadi *et al*., 2020). These interactions highlight the importance of region-specific analyses in understanding the mechanisms that govern crustal deformation in West Java.

Researchers determine the dominant stress regime by calculating the stress ratio (R), which quantifies the relative magnitudes of the principal stresses (σ_1, σ_2, σ_3) (see Equation 1) (Gephart and Forsyth, 1984). This ratio indicates whether the stress state in a region involves extensional, compressional, or shear deformation (Zoback, 1992).

$$R = \frac{\sigma_1 - \sigma_2}{\sigma_1 - \sigma_3} \quad \text{.....(1)}$$

Understanding stress ratios and orientations in detail enables one to assess faults and evaluate seismic risk more accurately. These measurements may also provide valuable insights for the implementation of safe practices within the geo-energy sectors, encompassing geothermal, oil, and gas operations (Zoback, 1992; Zoback, 2007). Through geomechanical assessments that incorporate stress factors, it is possible to predict strain energy build-up along fault lines (Scholz, 2002; Ellsworth, 2013), to determine fault criticality, and to develop effective mitigation strategies to reduce the impacts of earthquakes. A detailed analysis of stress ratios and orientations play a crucial role in assessing earthquake potential, as these factors directly control how strain accumulates and releases across faults (Palgunadi *et al*., 2020; 2024).

Existing studies have merely focused on stress changes caused by individual seismic or volcanic events (Gunawan *et al*., 2019; Marliyani *et al*., 2020). However, these studies often overlook the broader, ongoing stress conditions and fail to account for the influence of local geological structures. Pratama and Kita (2022) have provided a detailed map of regional stress orientations resulting from subduction, as shown in Figure 1. Nevertheless, this map does not include information on local stress variations.

The SHmax ranges from -1 (normal fault) to 1 (thrust fault), with 0 indicating strike-slip faults. The tectonics of the Indonesian Subduction Zone primarily forms from the interaction between the Indo-Australian Plate in the west, which has a slip rate of 5–6 cm/yr, and the Pacific Plate in the east, which has a slip rate of 7−8 cm/yr. The SHmax data were collected from a previous study by Pratama and Kita (2022), and have been modified.

Existing studies provide insights into the stress changes triggered by individual events and their immediate impact on the surrounding geological structures. However, they lack a clear resolution and a comprehensive analysis of ongoing stress conditions across West Java. This study addresses that gap by mapping stress ratios, principal stress orientations, and identifying the overall stress regimes across West Java using an advanced iterative joint inversion method. The iterative Joint inversion approach simultaneously inverts both the stress tensor and fault orientations from focal mechanisms. This method was selected for its demonstrated ability to accurately resolve stress orientations and ratios from moment tensor and focal mechanism data, even in the complex tectonic settings of West Java, where subduction

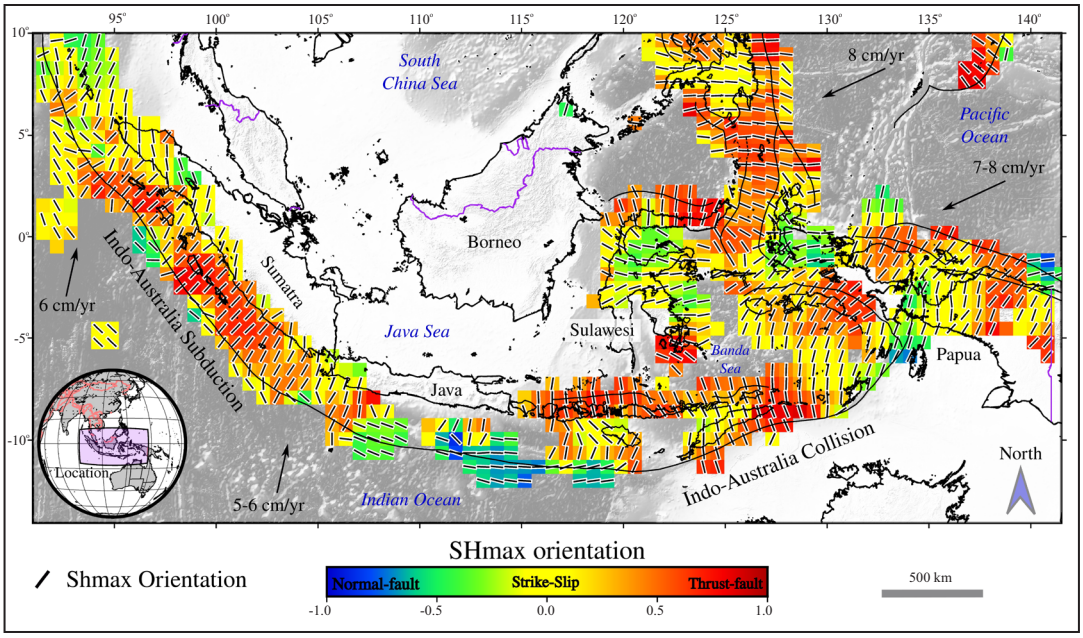

Figure 1. Spatial mean of SHmax orientation and fault type in The Indonesian Archipelago.

dynamics and geological heterogeneity create highly complicated stress patterns.

This study provides a detailed mapping of stress conditions, significantly enhancing seismic hazard assessments and enabling more informed mitigation strategies for West Java densely populated and earthquake-prone regions. Stress inversion of a total of 232 moment tensors and focal mechanisms in West Java reveals a transition from low stress ratios (R = 0.08–0.3) in sedimentary basins to high ratios (R= 0.8–0.97) in the fore-arc, demonstrating subduction-driven compression resulting from slab dehydration. Shallow normal faulting characterizes the southeastern region, sharply contrasting with the dominant reverse/oblique faulting in the fore-arc. Depth-dependent stress transitions and localized extensions near Mount Anak Krakatau highlight the interplay between subduction dynamics and volcanic processes.

Data and Methods

Data

Moment tensor (MT) data were analyzed spanning from 1976 to July 2024 to determine the spatial stress ratio and principal stress orientations in the West Java region. The MT dataset was compiled from the Global Centroid Moment Tensor Project (GCMT) and the International Seismological Centre (ISC). Figure 2 illustrates that the MT data encompasses a wide range of depths and magnitudes. The final dataset comprises 331 MT events, before event filtering, with magnitudes ranging from M4.3 to M6.7, representing a broad spectrum of moderate to significant earthquakes. The focal depths of these events range from 12 km to 157 km, documenting seismic activity across both shallow and intermediate-depth zones.

Methods

First, the spatial location of the moment tensor (MT) data was categorised into multiple clusters using DBSCAN (Density-Based Spatial Clustering) (Ester *et al.*, 1996; Schubert *et al.*, 2017) before performing stress inversion. This robust clustering algorithm, widely used in spatial data analysis and earthquake clustering, allows us to partition the data more effectively. Unlike conventional methods, DBSCAN identifies clusters based on local density distribution within a defined neighbourhood, without eliminating the need to specify the number of clusters in advance. This process is precisely controlled using two parameters: ε (epsilon) which determines the

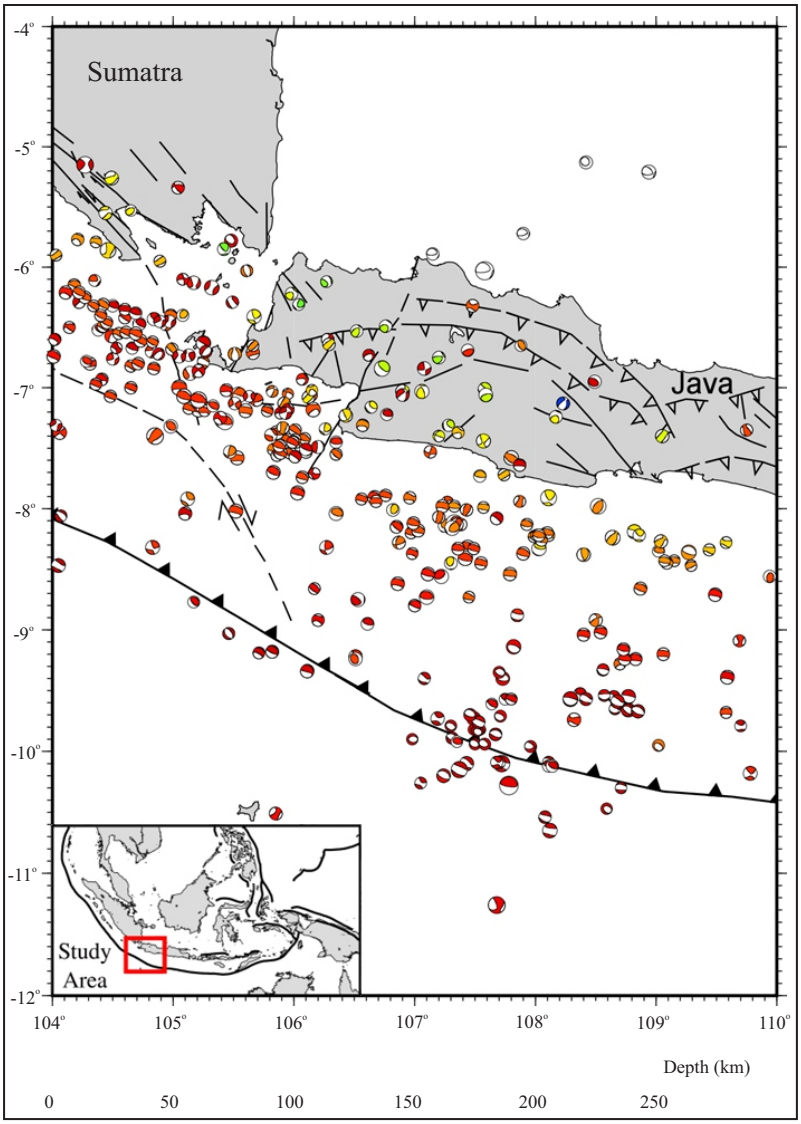

Figure 2. The distribution of available moment tensor (MT) solutions for events in western Java, based on data from the Global CMT catalog. The MTs were plotted according to their depth, using white focal mechanisms to represent events deeper than 250 km. Black lines mark the surface traces of documented faults, as identified by PuSGeN (2017).

neighbourhood radius, and MinPts which specifies the minimum number of points required to form a dense cluster. This approach enables the detection of geometrically complex clusters. Furthermore, DBSCAN enhances clustering clarity by automatically classifying labeling outliers as noise, thereby facilitating the distinction of meaningful patterns from scattered, geophysically insignificant data (Xu and Tian, 2015).

DBSCAN was applied to analyze the dataset of 331 moment tensor (MT) solutions, identifying clusters by setting a neighbourhood radius (ε) of 0.2° (~20 km) and a minimum of three data points (MinPts). This radius defines the maximum distance between two points for them to be considered part of the same cluster, with points within ε designated as neighbours (Ester *et al*., 1996). The cluster analysis was identified multiple groups based on these criteria, while rejecting eighty-nine events that did not satisfy the minimum density conditions as noise. These noise events represent outliers or sparsely distributed occurrences that DBSCAN excluded from cluster assignment according to the defined parameters.

To conduct a more detailed analysis, the events were stratified within each cluster into subsets by

focal depth: h ≤ 30 km for shallow crustal earthquakes, 30 km < h ≤ 60 km for subduction interface earthquakes, and h > 60 km for subduction intraslab earthquakes. This depth-based stratification was implemented to assess variations in fault types and their orientations across different depth ranges within individual clusters. After applying all selection criteria, 232 events were retained for analysis, organized into twenty-three clusters (Figure 3). Figure 3a shows the spatial distribution of these clusters, while Figure 3b illustrates their depth distribution. Cluster sizes exhibit an extensive range, from two to eighty events.

After clustering and selecting events, the iterative joint inversion technique was applied using the StressInversion code (Vavryčuk, 2014) to determine stress and fault orientations simultaneously. This method combines earthquake focal mechanisms to resolve stress tensor orientations and fault geometries concurrently, significantly enhancing the accuracy of stress regime reconstructions. The technique precisely estimates key stress parameters, including the orientations of the three principal stress axes (σ_1, σ_2, σ_3) and their relative magnitudes. The StressInversion code processes input data of strike, dip, and rake (derived from moment tensor solutions) to calculate regional stress parameters. The output graphically represents the principal stresses (σ_1, σ_2, σ_3) and the shape ratio (R), which quantifies the stress regime.

The value of R characterizes the stress ellipsoid: a low R (near 0) corresponds to $\sigma_1 > \sigma_2 \approx \sigma_3$, indicating anisotropic stress conditions, while a high R (near 1) reflects $\sigma_2 \approx \sigma_3 > \sigma_1$, suggesting more isotropic stress conditions (Zoback, 1992). An anisotropic compression typically leads to reverse faulting or strike-slip faulting, depending on the orientation of the anisotropy relative to the principal stresses. An isotropic stress condi-

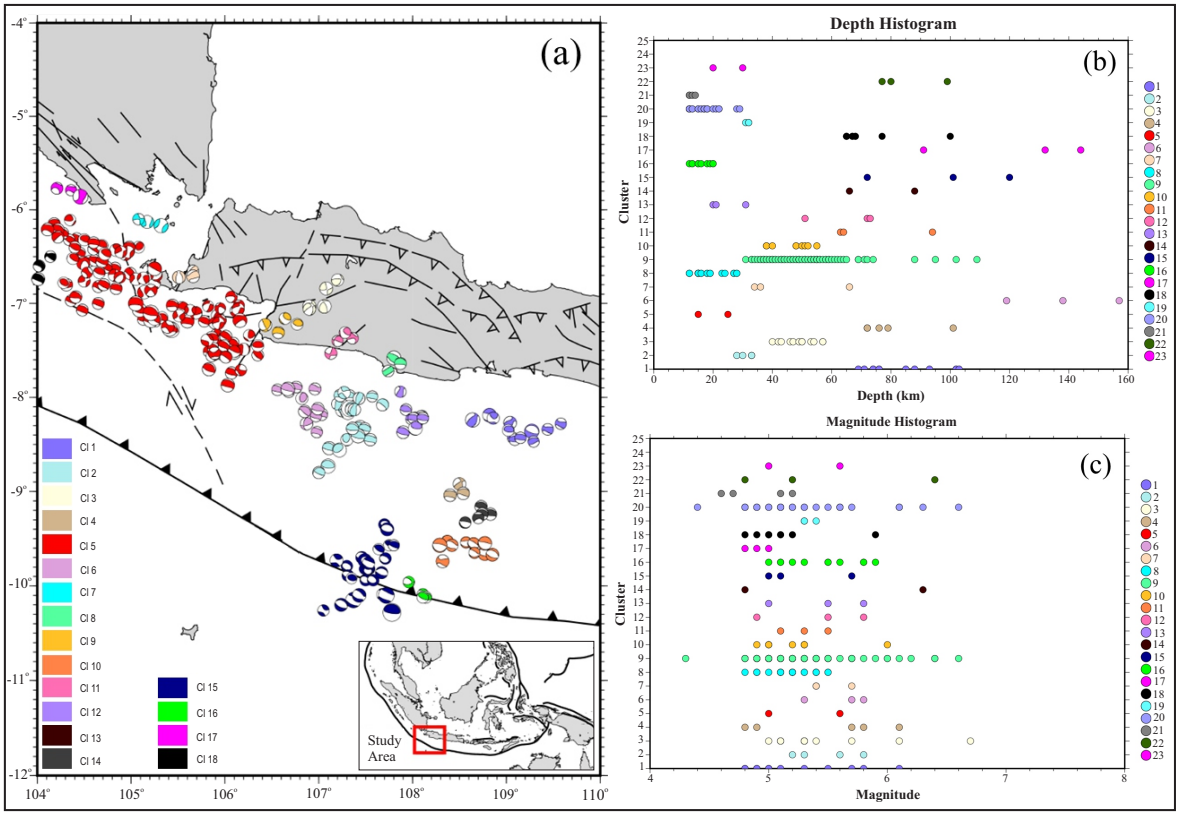

Figure 3. (a) The map illustrates the distribution of moment tensor (MT) clusters across western Java. The colours representing the focal mechanisms indicate the cluster IDs determined from the DBSCAN results. (b) This panel displays a depth histogram showing the events organized by each cluster. (c) Here, a magnitude histogram is presented detailing the events within each cluster.

tion can lead to strike-slip or normal faulting, depending on the orientation of the fabrics with respect to the principal stresses. Intermediate values (~0.5) represent transitional regimes. This parameter effectively distinguishes spatial variations in tectonic loading, such as the contrast between compression driven by subduction and localized extension (Michael, 1987; Gephart and Forsyth, 1984). Figure 4 presents representative results from three of the twenty-three stress inversions in western Java. Two key factors assess the reliability of these solutions: (1) confidence in the orientations of principal stress axes, a primary quality indicator, and (2) distinct histogram patterns of shape ratios (R) that validate the consistency of stress magnitudes across clusters. This integrated evaluation of axis confidence and histogram clarity provides robust assessments of stress conditions, thereby yielding more reliable tectonic interpretations in the region.

In the final stage of our analysis, the stress regime was determined to characterize the stress conditions in the studied area, specifically whether they are compressional, extensional, or shear. The prevailing stress regime was classified based on the stress inversion results, following

Cluster 1	
Number of events	12
Lon/Lat Centroid	109.11/-8.34
σ_1 (Plunge/Azimuth)	3.72/136.89
σ_2 (Plunge/Azimuth)	1.90/226.93
σ_3 (Plunge/Azimuth)	85.82/343.96
Stress-Ratio (R)/Friction	0.28/0.50
Principal Mechanism	49.59/35.48/93.28
Stress-Regime	Reverse (R)

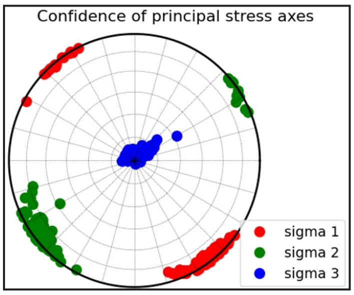

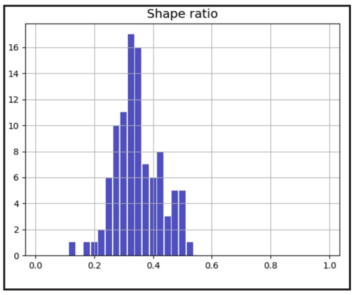

Cluster 8	
Number of events	26
Lon/Lat Centroid	105.20/-6.85
σ_1 (Plunge/Azimuth)	24.31/204.19
σ_2 (Plunge/Azimuth)	58.21/67.40
σ_3 (Plunge/Azimuth)	19.19/303.23
Stress-Ratio (R)/Friction	0.78/0.50
Principal Mechanism	61.54/86.38/31.60
Stress-Regime	Strike-slip (SS)

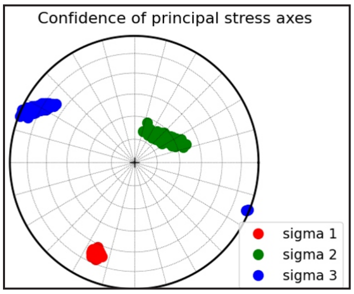

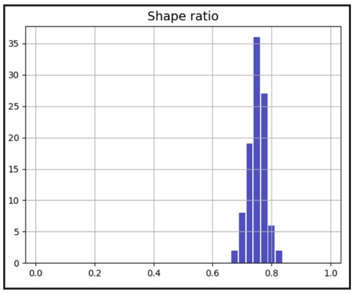

Cluster 20	
Number of events	27
Lon/Lat Centroid	107.53/-9.86
σ_1 (Plunge/Azimuth)	63.30/242.56
σ_2 (Plunge/Azimuth)	16.65/116/06
σ_3 (Plunge/Azimuth)	20.24/19.73
Stress-Ratio (R)/Friction	0.39/0.95
Principal Mechanism	296.65/88.02/-73.34
Stress-Regime	Normal (N)

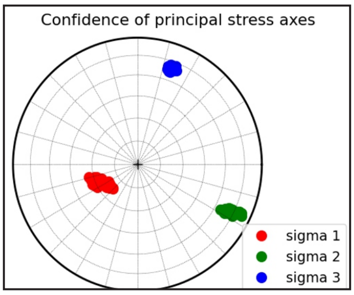

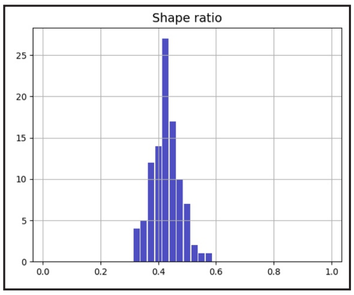

Figure 4. The stress inversion results of clusters CL5, CL11, and CL17 exhibit principal stress orientations and magnitudes. The confidence parameters confirm the reliability of the σ_1, σ_2, and σ_3 orientations. The stress ratio (R) was calculated for each cluster using shape ratio histograms, which represent the relative magnitudes of the principal stresses.

Zoback's 1992 methodology (see Table 1). The findings indicate that the cluster exhibits normal faulting (N), reverse faulting (R), strike-slip faulting (SS), and oblique faulting (O).

Table 2 summarizes the stress inversion results for all clusters, presenting key parameters and findings. The stress ratio (R) varies significantly across clusters, ranging from 0.08 to 0.97. Simi-

Table 1. Classification of Stress Regime According to Zoback (1992) Classification (Pl= Plunge; σ_1= maximum principal compressive stress; σ_3= minimum principal compressive stress)

Plunge of Axes			Faulting Type
σ_1	σ_2	σ_3	
Pl ≥ 52º		Pl ≤ 35º	Normal (N)
40º ≤ Pl < 52º		Pl ≤ 20º	Normal with Strike-Slip component (N-SS)
Pl < 40º	Pl ≥ 45º	Pl ≤ 20º	Strike-Slip (SS)
Pl ≤ 20º	Pl ≥ 45º	Pl < 40º	Strike-Slip (SS)
Pl ≤ 20º		40º ≤ Pl < 52º	Reverse with Strike-Slip component (R-SS)
Pl ≤ 35º		Pl ≥ 52º	Reverse (R)
25º < Pl < 45º	25º < Pl < 45º	25º < Pl < 45º	Oblique faulting (O)
40º < Pl < 50º	40º < Pl < 50º	40º < Pl < 50º	

Table 2. Summary of Stress Inversion Results And Stress Regime of Each Cluster in West Java Region Classification regime type N: Normal; SS: Strike-slip; R: Reverse; SS: Strike-slip; O: unknown or oblique faulting

Cluster ID	Number of Events in Cluster	Centroid Coordinate		σ_1		σ_2		σ_3		Stress Ratio (R)	Friction	Stress Regime
		Longitude	Latitude	Azimuth	Plunge	Azimuth	Plunge	Azimuth	Plunge			
1	12	109.11	-8.34	136.80	3.72	226.93	1.90	343.96	85.82	0.28	0.50	R
2	4	107.11	-8.66	216.45	12.33	110.92	50.78	315.77	36.52	0.48	0.75	SS
3	12	107.37	-8.19	87.65	7.04	178.90	10.03	323.16	77.70	0.37	0.60	R
4	5	107.35	-8.14	231.00	30.03	133.94	12.01	24.68	57.19	0.35	0.95	R
5	2	106.99	-6.95	206.05	22.11	20.88	67.81	115.32	1.81	0.31	0.40	SS
6	3	107.05	-6.94	309.15	0.02	219.15	7.67	39.32	82.33	0.33	0.40	R
7	3	108.48	-8.99	277.37	13.12	168.23	54.58	15.82	32.22	0.21	0.50	SS
8	26	105.20	-6.85	204.19	24.31	67.40	58.21	303.23	19.19	0.78	0.50	SS
9	80	105.28	-6.99	199.71	23.62	290.18	1.07	22.63	66.35	0.79	0.55	R
10	9	106.83	-8.08	198.47	23.76	301.43	27.00	73.28	52.62	0.90	0.45	R
11	3	106.88	-8.07	87.19	21.96	183.44	15.12	305.27	62.88	0.96	0.85	R
12	3	105.61	-6.69	117.76	35.79	5.69	27.53	247.91	41.81	0.97	0.95	O
13	3	105.19	-6.13	32.16	53.80	243.97	31.88	144.15	15.33	0.33	0.80	N
14	2	107.77	-7.65	286.81	5.53	17.66	8.70	164.75	79.67	0.08	0.40	R
15	3	106.55	-7.23	203.51	55.20	96.97	11.19	359.74	32.46	0.40	0.40	N
16	11	108.62	-9.59	233.18	74.96	115.79	7.05	24.13	13.22	0.61	0.75	N
17	3	107.28	-7.36	186.91	25.15	335.83	61.27	90.70	12.98	0.88	0.40	SS
18	9	108.04	-8.22	191.31	29.16	98.40	5.18	359.26	60.30	0.85	0.70	R
19	3	108.77	-9.21	196.41	26.22	287.71	2.64	23.04	63.63	0.62	0.40	R
20	27	107.53	-9.86	242.56	63.30	116.06	16.65	19.73	20.24	0.39	0.95	N
21	4	108.08	-10.07	194.40	61.34	293.68	5.04	26.39	28.13	0.89	0.95	N
22	3	104.34	-5.81	187.72	42.24	298.57	21.41	47.85	40.10	0.65	0.95	O
23	2	104.02	-6.67	206.42	31.86	111.51	7.84	9.28	56.96	0.68	0.40	R

larly, the friction coefficient exhibits substantial variation, with values ranging from 0.40 to 0.95. The clusters exhibit diverse stress regimes, including normal faulting (NF), strike-slip faulting (SS), reverse faulting (RF), and oblique faulting (OF).

Results and Analysis

The stress inversion results reveal a complex spatial pattern of crustal stress across West Java, characterized by systematic variations in the stress ratio (R). Stress ratio values range from 0.08 in central sedimentary basins to 0.97 in the fore-arc region (Figure 5). A progressive increase was observed from basin areas (R= 0.08–0.3) toward the fore-arc (R= 0.8–0.97).

The observed stress distribution illustrates how three key tectonic processes dynamically interact: (1) slab bending dynamics where alternating tension and compression occur as plates bend and unbend, transitioning to down-dip compression at depth (Hasegawa *et al.*, 1994; Ranero *et al.*, 2003, 2005); and (2) fluid-related weakening through metamorphic dehydration at intermediate depths, which reduces the strength of the plate interface (Koulakov *et al.*, 2009; Ranero *et al.*, 2003). This complex interaction produces distinct stress regimes in the region. Central basins exhibit low R values (0.08-0.3) at depths below 60 km, likely due to metamorphic dehydration at this depth (Koulakov *et al.*, 2009), while the fore-arc experiences elevated stresses (R= 0.8-0.97) resulting from strong interplate coupling (Scholz and Campos, 2012), active fault

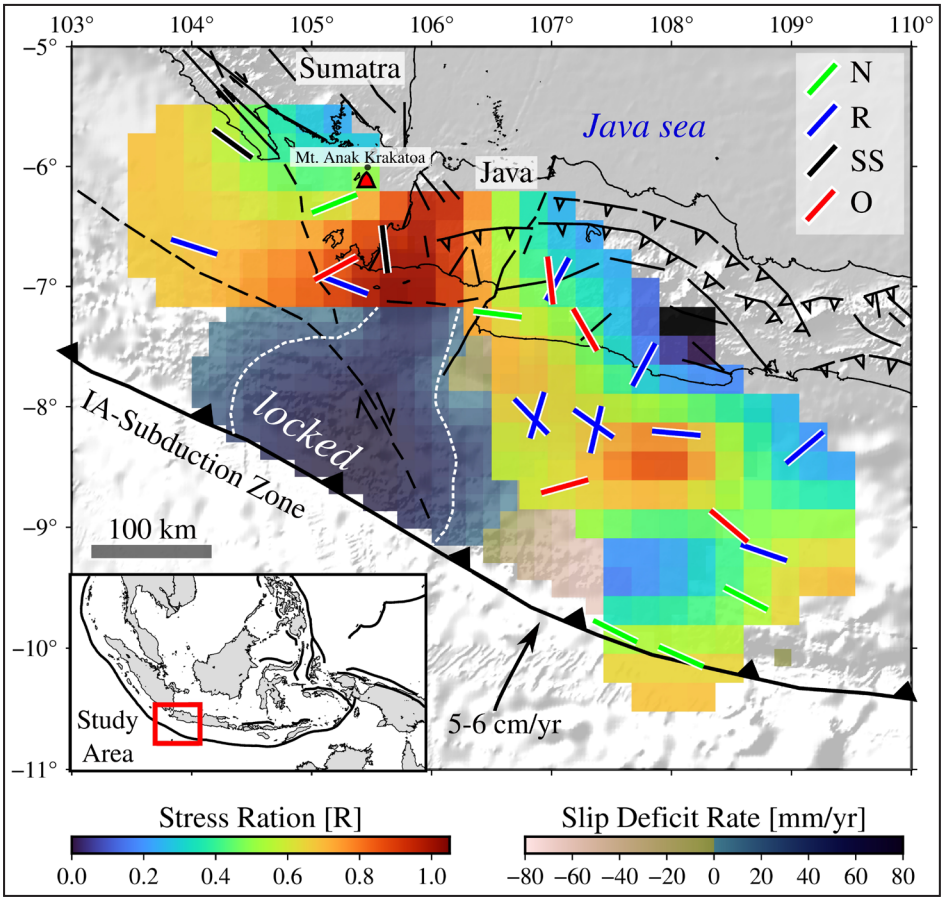

Figure 5. The stress ratio (R) and stress regimes (represented by coloured lines in West Java derived from the stress inversion analysis. The stress regimes were classified as follows: N (normal), R (reverse), SS (strike slip), and O (oblique). For comparative analysis, the slip deficit map was overlaid from Hanifa *et al.* (2014). The southesternmost part of Java Island exhibits the highest stress ratio values (R ≈ 1)

systems, and rheological contrasts between The Sunda Shelf basement and the accreted sediments (Townend and Zoback, 2000). Collectively, these systematic stress variations record the mechanical evolution of the subduction system, progressing from initial slab bending to deep fluid-mediated weakening processes. Figure 5 also incorporates the slip deficit map from Hanifa *et al*. (2014). The distribution of stress ratios shows strong alignment with GPS-derived coupling estimates, confirming that areas with high plate coupling (50−90 %) consistently correspond to zones of fault instability and dominant horizontal stress. A locked asperity pushes the hanging wall vertically and laterally. This correlation suggests that these regions may serve as normal or strike-slip partitioning or transpressional convergence.

In addition, regions with high plate coupling exhibit low stress ratio ($R < 0.3$), which do not indicate weak or extensional stress. Low R reflects a highly anisotropic stress ellipsoid where σ_1 strongly dominates ($\sigma_1 >> \sigma_2 \approx \sigma_3$), signifying intense directional compression in locked asperities (Michael, 1987; Zoback, 1992; McCaffrey, 2009). This condition promotes stress partitioning and heterogeneous deformation: reverse or strike-slip motion dominates in the asperity core, while stress rotation, bending, and flexural rebound at the margins generate normal or transpressional faulting (Townend and Zoback, 2000; Ranero *et al*., 2003; Koulakov *et al*., 2009; Simanjuntak *et al*., 2025). Low R in these high-coupling zones, this represents strong compressional anisotropy and strain accumulation, consistent with active transpressional deformation along the Java fore-arc.

The investigation reveals an unexpected concentration of normal faulting (N) stress regimes in the southeasternmost segment of the studied area, precisely coinciding with the zone where the oceanic plate subducts beneath the continental margin (Clusters 20 and 21, Figure 5). The observed SHmax orientations are consistently aligned WNW−ESE, parallel to the subduction trench axis, which strongly suggests trench-parallel extension. This finding validates Pratama and Kita (2022), who documented similar normal faulting regimes in Java. Notably, normal fault (N) stress regimes was observed at shallow depths (<30 km) along the subduction interface. These regimes arise from four primary mechanism (i) localized bending stresses as the slab steepens its descent into the mantle (Ranero *et al*., 2003; Ranero *et al*., 2005), (ii) transient stress release following major seismic events (Imanishi *et al*., 2012), (iii) fluid overpressures along permeable fault strands within the subduction channel (Koulakov *et al*., 2009; Saffer and Tobin, 2011), and (iv) the subducting seamounts/ridges that create local stress perturbations (Kopp *et al*., 2006; Wang and Bilek, 2011; Mochizuki *et al*., 2008). The shallow-depth normal fault (NF) stress regimes in this study, at depths of less than 30 km, most likely reflect seamount-induced stress perturbations, consistent with the Bassett and Watts (2015) model of flexural plate bending.

The fore-arc region of eastern West Java exhibits pronounced spatial and depth-dependent variations in stress regimes, highlighting the dynamic interplay between regional tectonic forces and local structural controls. The area is primarily characterized by reverse (R) and oblique (O) faulting regimes, marking a transition from compressional to strike-slip deformation. The oblique regimes feature mixed reverse-strike-slip (R-SS) and normal-strike-slip (N-SS) components. Near the trench (Cluster 16, Figure 5), a distinct normal faulting (N) stress regime was identified, spatially correlated with similar extensional events that appear to be influenced by plate bending and fluid overpressure effects (Ranero *et al*., 2003, 2005).

The analysis reveals near-orthogonal differences in maximum horizontal stress (SHmax) orientations between adjacent clusters specifically, between the overriding plate in cluster 3 and the subducting slab in cluster 4, as well as between cluster 10 (the overriding plate), and cluster 11 (the subducting slab). Notably, while all clusters exhibit a reverse fault stress regime at intermediate depths, their distinct tectonic settings produce contrasting stress patterns. Significant variations in SHmax orientation was documented between

the 30–60 km and >60 km depth ranges, indicating a depth-dependent stress rotation. A dynamic interplay between the overriding plate and subducting slab best explains these near-orthogonal differences (Figure 5). The overriding plate experiences compression from plate coupling (Scholz and Campos, 2012), while the subducting slab re-orients stresses with depth through bending or unbending processes (Christova and Scholz, 2003).

The analysis of the coastal West Java region reveals distinct variations in stress regimes across shallow depths (≤30 km) and intermediate depths (>30 km), characterized by reverse (R) and oblique (O) faulting. The dominance of reverse faulting indicates the presence of compressional stress generated by subduction-related tectonic loading. Furthermore, oblique faulting mechanisms (normal or reverse strike-slip) indicate a superimposed horizontal shear component, potentially resulting from either oblique plate convergence or structural heterogeneity along the plate interface, including seamount collision or fracture zone subduction (Kopp *et al*., 2006, 2009; Simons *et al*., 2007). The observed orientations of SHmax falls into two principal directions: WNW−ESE and NE−SW. The WNW−ESE orientations align with trench compression, while the NE−SW directed stresses correspond to slab bending processes. These findings are consistent with the faulting patterns identified along the Java Trench by Kopp *et al*. (2006, 2009).

The island arc exhibits complex variations in stress regimes at intermediate depths, characterized by the coexistence of normal (N), reverse (R), and oblique (O) faulting stress regimes. Normal faulting reflects localized extensional stresses, potentially associated with slab unbending (Hasegawa *et al*., 1994) or fluid-induced hydration due to slab bending (Ranero *et al*., 2003; Ranero *et al*., 2005) of the subducting Indo-Australian slab as it descends beneath The Eurasian Plate, generating tension in the overriding plate. In this normal faulting stress regime, the SHmax orientation follows in an ENE–SSW direction.

The reverse faulting stress regime beneath the island arc primarily arises from strong plate coupling, which transfers compressional stresses to intermediate depths, as described by Scholz and Campos (2012). Alternatively, it may arise from slab dehydration that raises pore pressures, as observed in Central Java by Koulakov *et al*. (2009). The oblique faulting, comprising both normal- and reverse-strike-slip components, indicates significant stress partitioning, strongly influenced by sharp slab bending and abundant fluid release (Koulakov *et al*., 2009). This condition leads to a transitional regime where normal and reverse faulting mechanisms can occur simultaneously. Furthermore, along-strike variations in slab geometry and subducting seamounts (Kopp *et al*., 2009) may locally modify the stress field, promoting complex fault kinematics.

A normal fault mechanism (N) is observed in the vicinity of Mount Anak Krakatau, confirming that extensional tectonic forces are actively deforming the region. This type of faulting provides clear evidence that the crust is undergoing extension, primarily driven by regional tectonics and potentially amplified by volcanic activity linked to the subduction of the Indo-Australian Plate beneath the Eurasian Plate. Source mechanism studies by Iguchi *et al*. (2001) and Mahbub *et al.* (2023) strongly support these findings, consistent with the extensional stress regime around Mount Anak Krakatau identified in stress analyses by Marliyani *et al*. (2020).

The 232 moment tensor data from the global catalogue offers fundamental insights into stress ratios and stress regimes across West Java. However, the data set remains limited due to its incomplete coverage. Moment tensor data have not yet been integrated from local catalogues or studies, which typically provide higher resolution and region-specific insights. A comprehensive synthesis of these local datasets would significantly enhance the accuracy of stress analysis, enabling a more robust characterization of the area stress regimes. Such integration constitutes a crucial step in developing a precise representation of the region's tectonic dynamics.

Conclusions

Analysis of 232 earthquake moment tensors reveals valuable insights into the stress patterns within the tectonic setting of West Java. The results show significant variations in the stress ratio, SHmax orientation, and types of stress regimes across the region.

The stress ratio distribution in West Java varies significantly, ranging from 0.08 to 0.97. Central sedimentary basins exhibit stress ratios (R) between 0.08 and 0.3, whereas the fore-arc shows much higher stress ratios, ranging from 0.8 to 0.97. Sedimentary basins and coastal zones contribute to the lower stress ratios by exhibiting reduced tectonic compression. In contrast, increased tectonic activity drives the rise in stress ratios toward the fore-arc, as does fluid release from slab dehydration.

A shallow normal faulting regime (<30 km) in southeastern West Java shows extensional stress, likely reflecting localized stress perturbations.

The fore-arc region of eastern West Java exhibits a variety of stress regimes, primarily characterized by reverse (R) and oblique (O) faulting. Subduction dynamics actively interact with local structural heterogeneities to shape these conditions.

Stress regimes exhibit depth-dependent transitions in coastal and island-arc regions. The regime combines reverse (R), strike-slip (SS), and oblique (O) faulting, which indicates a compressional environment with significant horizontal shear.

Near Mount Anak Krakatau, extensional tectonic forces indicated by a normal fault (N) mechanism likely arises from regional tectonics or volcanic activity resulting from the subduction of the Indo-Australian Plate.

Acknowledgments

This research was funded by the HETI ADB Loan INO-4110, 2024, as part of the Indonesian Collaborative Research scheme, Institut Teknologi Sepuluh November, Surabaya. The authors also acknowledge financial support from Universitas Indonesia with contract number NKB-771/UN2.RST/HKP.05.00/2024 and from Universitas Gadjah Mada with contract number 1920/UN1/DITLIT/PT.01.03/2024. All figures were created in GMT v.6 (Wessel *et al*., 2019).

References

Bassett, D. and Watts, A.B., 2015. Gravity anomalies, crustal structure, and seismicity at subduction zones: 2. Interrelationships between fore-arc structure and seismogenic behavior, *Geochemistry Geophysics Geosystems,* 16, P.1541-1576. DOI:10.1002/2014GC005685.

Christova, C. and Scholz, C., 2003. Stresses in the Vanuatu Subducting Slab: a test of two hypotheses. *Geophysical Research Letters,* 30, 10.1029/2003GL017701.

Ellsworth, W.L., 2013. Injection-induced earthquakes. *Science,* 341 (6142), 1225942. DOI: 10.1126/science.1225942.

Ester, M., Kriegel, H.P., Sander, J., and Xu, X., 1996. A density-based algorithm for discovering clusters in large spatial databases with noise. *KDD,* 96 (34), p.226-231.

Gephart, J.W. and Forsyth, D.W., 1984. An improved method for determining the regional stress tensor using earthquake focal mechanism data: application to the San Fernando earthquake sequence, *Journal of Geophysical Research,* 89, p.9305-9320.

Gunawan, E., Widiyantoro, S., Marliyani, G.I., Sunarti, E., Ida, R., and Gusman, A.R., 2019. Fault source of the 2 September 2009 Mw 6.8 Tasikmalaya intraslab earthquake, Indonesia: Analysis from GPS data inversion, tsunami height simulation, and stress transfer. *Physics of the Earth and Planetary Interiors*, 291, p.54-61.

Hanifa, N.R., Sagiya, T., Kimata, F., Efendi, J., Abidin, H.Z., and Meilano, I., 2014. Interplate coupling model off the southwestern coast of Java, Indonesia, based on continuous GPS data in 2008-2010, *Earth and Planetary Science Letters,* 401, p.159-171, ISSN 0012- 821X, https://doi.org/10.1016/j.epsl.2014.06.010.

Harjono, H., Diament, M., Dubois, J., Larue, M., and Deplus, C., 1991. Seismicity of the Sunda Strait: Evidence for Crustal Extension and Volcanological Implications. *Tectonics,* 10 (1), p.17-30.

Hasegawa, A., Horiuchi, S., and Unimo, N., 1994. Seismic structure of the northeastern Japan convergent margin: A synthesis. *Journal of Geophysical Research,* 99 (B11), 22,295-22,311. DOI:10.1029/93JB02797.

Iguchi, M., Suantika, G., Sulaeman, C., Wildan, A., Sutawidjaja, I.S., Kriswati, E., ... and Surono, T.H., 2001. *Source Mechanisms of Volcanic Earthquakes at Some Volcanoes in Indonesia,* Bandung.

Imanishi, K., Ando, R., and Kuwahara, Y., 2012. Unusual shallow normal-faulting earthquake sequence in compressional northeast Japan activated after the 2011 off the Pacific coast of Tohoku earthquake, *Geophysical Research Letters,* 39, L09306. DOI: 10.1029/2012GL051491.

Kopp, H., Hindle, D., Klaeschen, D., Oncken, O., Reichert, C., Scholl, D., 2009. Anatomy of the western Java plate interface from depth-migrated seismic images. *Earth and Planetary Science Letters,* 288 (3-4), p.399-407. DOI:10.1016/j.epsl.2009.09.043.

Kopp, H., Flueh, E., Petersen, C.J., Weinrebe, W., and Wittwer, A., 2006. The Java margin revisited: Evidence for subduction erosion off Java. *Earth and Planetary Science Letters*, *242*, p.130-142. DOI:10.1016/j.epsl.2005.11.036.

Koulakov, I., Bohm, M., Asch, G., Lühr, B.-G., Manzanares, A., Brotopuspito, K.S., Fauzi, Purbawinata, M.A., Puspito, N.T., Ratdomopurbo, A., Kopp, H., Rabbel, W., and Shevkunova, E., 2009. P and S velocity structure of the crust and the upper mantle beneath central Java from local tomography inversion, *Journal of Geophysical Research,* 112, B08310, DOI:10.1029/2006JB004712.

Koulali, A., Susilo, S., McClusky, S., Meilano, I., Cummins, P. R., Tregoning, P., ... and Efendi, J., 2017. The Kinematics of Crustal Deformation in Java from GPS Observations: Implications for Fault Slip Partitioning. *Journal of Geophysical Research: Solid Earth,* 122 (8), p.6617-6638.

Mahbub, R.M., Ragil, C., and Qoyyibi, D.S., 2023. Indications of a transtensional strike-slip fault at Mount Anak Krakatau, based on earthquake focal mechanism data. *IOP Conference Series: Earth and Environmental Science* 1151.

Marliyani, G.I., Helmi, H., Arrowsmith, J.R., and Clarke, A., 2020. Volcano morphology as an indicator of stress orientation in the Java Volcanic Arc, Indonesia. *Journal of Volcanology and Geothermal Research*, 400, 106912.

McCaffrey, R., 2009. The tectonic framework of the Sumatran subduction zone, *Annual Review of Earth and Planetary Sciences,* 37, 3.1–3.22.

Michael, A.J., 1987. Use of focal mechanisms to determine stress: A control study. *Journal of Geophysical Research*, 92 (B1), p.357-368, DOI:10.1029/JB092iB01p00357.

Mochizuki, K., Yamada, T., Shinohara, M., Yamanaka, Y., and Kanazawa, T., 2008. Weak interplate coupling by seamounts and repeating M ~ 7 earthquakes, *Science,* 321 (5893), 1194-7. DOI:10.1126/science.1160250.

Palgunadi, K.H., Gabriel, A.A., Garagash, D.I., Ulrich, T., and Mai, P.M., 2024. Rupture dynamics of cascading earthquakes in a multiscale fracture network. *Journal of Geophysical Research: Solid Earth*, 129 (3), P????-????. DOI:e2023JB027578.

Palgunadi, K.H., Gabriel, A.A., Ulrich, T., López-Comino, J.Á., and Mai, P.M., 2020. Dynamic Fault Interaction during a Fluid-Injection-Induced Earthquake: The 2017 Mw 5.5 Pohang Event. *Bulletin of the Seismological Society of America*, 110 (5), p.2328-2349. DOI:10.1785/0120200106.

Pratama, W. and Kita, S., 2022. Stress field orientation obtained from earthquake focal mechanisms in Indonesia region, Synopsis of IISEE-GRIPS Master Thesis.

Pusat Studi Gempa Nasional (PuSGeN), 2017. Peta Sumber dan Bahaya Gempa Indonesia

Tahun 2017. *Indonesia Earthquake Source and Hazard Map,* Kementerian Pekerjaan Umum dan Perumahan Rakyat.

Ranero, C.R., Villaseñor, A., Morgan, J.P., and Weinrebe, W., 2005. Relationship between bend-faulting at trenches and intermediate-depth seismicity, *Geochemistry Geophysics Geosystems,* 6, Q12002, DOI:10.1029/2005GC000997.

Ranero, C.R., Morgan, J., Mcintosh, K., and Christian, R., 2003. Bending-related faulting and mantle serpentinization at the Middle America trench. *Nature,* 425, p.367-373. DOI:10.1038/nature01961.

Saffer, D.M. and Tobin, H.J., 2011. Hydrogeology and mechanics of subduction zone forearcs: fluid flow and pore pressure, *Annual Review of Earth and Planetary Sciences,* 39, p. 157-186. DOI:10.1146/annurev-earth-040610-133408.

Scholz, C.H. and Campos, J., 2012. The seismic coupling of subduction zones revisited. *Journal of Geophysical Research,* 117, B05310. DOI:10.1029/2011JB009003.

Schubert, E., Sander J., Ester, M., Kriegel, H.P., Xu, X., 2017. DBSCAN revisited: why and how you should (still) use DBSCAN. *ACM Trans Database Syst (TODS),* 42 (3), p.1-21. DOI:10.1145/3068335.

Simanjuntak, A.V., Palgunadi, K.H., Syaifuddin, F., Muksin, U., Riama, N.F., Sirait, A.M., ... and Warnana, D.D., 2025. Evidence of a new backthrust fault system from the 2022 southeast Java, Indonesia earthquake sequence: Insights from seismological analysis. *Journal of Asian Earth Sciences*, 106845. DOI:10.1016/j.jseaes.2025.106845.

Simons, W., Socquet, A., Vigny, C., Ambrosius, B.A.C., Abu, S., Promthong, C., Subarya, C., Sarsito, D., Matheussen, S., Morgan, P., and Spakman, W., 2007. A decade of GPS in Southeast Asia: Resolving Sundaland motion and boundaries. *Journal of Geophysical Research, 112*, DOI:10.1029/2005JB003868. 112. 10.1029/2005JB003868.

Townend, J. and Zoback, M.D., 2000. How faulting keeps the crust strong. *Geology,* 28 (5), p.399-402. DOI:10.1130/0091-7613(2000)28<399:HFKTCS>2.0.CO;2.

Vavryčuk, V., 2014. Iterative joint inversion for stress and fault orientations from focal mechanisms. *Geophysical Journal International*, 199 (1), p.69-77.

Wang, K. and Bilek, S.L., 2011. Do subducting seamounts generate or stop large earthquakes? *Geology*, 39 (9), p.819-822.

Wessel, P., Luis, J. F., Uieda, L., Scharroo, R., Wobbe, F., Smith, W. H. F., & Tian, D., 2019. The Generic Mapping Tools version 6. Geochemistry. *Geophysics, Geosystems*, 20, p.5556–5564. DOI:10.1029/2019GC008515

Xu, R. and Tian, Y., 2015. A comprehensive survey of clustering algorithms. *Annals of Data Science,* 2 (2), p.165-193. DOI:10.1007/s40745-015-0040-1.

Zoback, M.L., 1992. First- and second-order patterns of stress in the lithosphere: The World Stress Map Project, *Journal of Geophysical Research*, 97 (B8), p.11703-11728, DOI:10.1029/92JB00132.

Zoback, M.D., 2007. Reservoir Geomechanics. *Cambridge University Press*. DOI:10.1017/CBO9780511586477.